

1 Supplementary information of manuscript

2 **Evolution of source attributed organic aerosols and gases in a**
3 **megacity of central China**

4 Siyuan Li ¹, Dantong Liu ^{1,*}, Shaofei Kong ^{2,*}, Yangzhou Wu ¹, Kang Hu ¹, Huang Zheng ², Yi Cheng ²,
5 Shurui Zheng ², Xiaotong Jiang ¹, Shuo Ding ¹, Dawei Hu ³, Quan Liu ⁴, Ping Tian ⁵, Delong Zhao ⁵,
6 Jiujiang Sheng ⁵

7 ¹Department of Atmospheric Sciences, School of Earth Sciences, Zhejiang University, Hangzhou 310027, China

8 ²Department of Atmospheric Sciences, School of Environmental Studies, China University of Geosciences, Wuhan, 430074,
9 China

10 ³Centre for Atmospheric Sciences, School of Earth and Environmental Sciences, University of Manchester, Manchester M13
11 9PL, UK

12 ⁴State Key Laboratory of Severe Weather & Key Laboratory of Atmospheric Chemistry of CMA, Chinese Academy of
13 Meteorological Sciences, Beijing 100081, China

14 ⁵Beijing Key Laboratory of Cloud, Precipitation and Atmospheric Water Resources, Beijing Meteorological Service, Beijing
15 100089, P. R. China; Field Experiment Base of Cloud and Precipitation Research in North China, China Meteorological
16 Administration, Beijing 100089, P. R. China.

17

18 *Correspondence to:* Dantong Liu (dantongliu@zju.edu.cn); Shaofei Kong (kongshaofei@cug.edu.cn)

19

20

Table S1: The related coefficient between OA factors, marked profiles and VOC factors.

	HOA	COA	OOA1	OOA2	NO _x	BC	SO ₄ ²⁻	NO ₃ ⁻	O _x	Traffic VOCs	Cooking VOCs	SecVOC2	SecVOC1
HOA													
COA	0.285**												
OOA1	0.462**	0.666**											
OOA2	0.332**	-0.006	0.288**										
NO _x	0.708**	0.389**	0.321**	0.088*									
BC	0.834**	0.203**	0.453**	0.504**	0.672**								
SO ₄ ²⁻	0.335	0.106**	0.294**	0.821**	0.113**	0.478**							
NO ₃ ⁻	0.144**	-0.068	0.039	0.435**	0.075	0.399**	0.374**						
O _x	0.344**	0.228**	0.183**	0.700**	0.310**	0.444**	0.548**	0.113**					
Traffic VOCs	0.629**	0.305**	0.409**	0.159**	0.530**	0.534**	0.219**	0.124**	0.309**				
Cooking VOCs	0.564**	0.667**	0.698**	0.065	0.561**	0.487**	0.118**	-0.034	0.271**	0.522**			
SecVOC2	0.138*	-0.076	-0.033	0.673**	0.005	0.216**	0.381**	-0.126**	0.770**	0.026*	-0.18**		
SecVOC1	0.534**	0.667**	0.758**	0.124	0.474**	0.448**	0.179**	-0.063	0.121**	0.523**	0.746**	-0.11**	

21 **Correlation is significant at the 0.01 level (two-tailed)

22 * Correlation is significant at the 0.005 level (two-tailed)

23

24 **Text S1 PMF Analysis from HR-ToF-AMS.**

25 The HR-ToF-AMS mass spectrometer was operated under V-mode with high sensitivity ($m/\Delta m = \sim 2000$). The relative
26 ionization efficiencies (*RIEs*) of non-refractory species, i.e., sulfate, nitrate, chloride, and ammonium were determined to be
27 0.82, 1.1, 1.3, and 3.82, respectively.

28 The input data were the high-resolution organic mass spectral matrix of OA and the error matrix, and the Positive Matrix
29 Factorization (PMF) analysis was conducted using the PMF Evaluation Toolkit (PET) v2.08D. A minimum error value was
30 added to the error matrix and m/z with low signal-to-noise ($\text{SNR} < 0.2$) ratios are removed. But, those ions with “weak”
31 variables ($0.2 < \text{SNR} < 2$) are down-weighted by increasing the measurement errors by a factor of 2. The ions with m/z 19
32 and 20 are removed because of their negligible masses. Further, isotopes were removed since their signals are scaled to their
33 parent ions instead of being measured directly. The number of factors in the PMF solution was explored from 1 to 6. There
34 are several criteria that can be used to select the best modeled number of factors such as Q/Q_{exp} and the rotational parameter
35 (f_{peak}). The f_{peak} parameter can analyze the rotational ambiguity of the solution sets, and it was varied from -1 to 1 by a
36 step of 0.1. The Q -value corresponds to the number of the degrees of freedom of the fitted data: $Q_{\text{exp}} = tm - p(t + m)$, where t
37 and m is the dimensions of the matrix, p is the number of PMF factors, and $p(t + m)$ represent the free parameters of the
38 model. With the p increased, the Q decreased. The analysis used mass spectra consist of m/z 12 to 120 amu in this work. The
39 four-factor solution with $f_{\text{peak}} = 0$ and $Q/Q_{\text{exp}} = 3.04$ was chosen as the optimal solution according to the procedures
40 outlined in detail elsewhere Zhang et al. (2011).

41

42

43 Text S2 PMF Analysis from PTR-ToF-MS

44 The measurement error was tested based on the transmission gas and the benzene, toluene, styrene and xylenes in the
45 exhaust. The transmission calibration provided ratios for the normalized counts per second (ncps) per ppb(Hartikainen et al.,
46 2018). Comparison with the transmission calibrated ncps ppb⁻¹ values, the measurement concentration had 20-40%
47 uncertainty. Some reaction rates of VOCs with H₃O⁺ were based on the rates by Cappellin et al.(Cappellin et al., 2012) at
48 E/N 120, while the E/N was slightly higher (135 Td) in this experiment, which may result in underestimation of
49 concentrations.

50 Positive matrix factorization (PMF 5.0) is an advanced receptor model which decomposes an observation dataset ($i \times j$
51 dimensions) into three matrixes including factor contributions G ($i \times k$ dimensions), profiles matrix F ($k \times j$ dimensions), and
52 residue matrix E (e_{ij}):

$$53 \quad x_{ij} = \sum_{k=1}^p g_{ik} f_{kj} + e_{ij} \quad (1)$$

54 where x_{ij} is the concentration of j th species measured in i th sample, g_{ik} is the contribution of the k th source to the i th sample,
55 f_{kj} is the mass fraction of the j th compound in the k th source, and e_{ij} is the residual for each sample/species. The PMF
56 solution minimizes the target function Q according to the ratio of residual matrix (e_{ij}) elements and uncertainty (U_{ij}) as:

$$57 \quad Q = \sum_{i=1}^n \sum_{j=1}^m \left(\frac{e_{ij}}{U_{ij}} \right) \quad (2)$$

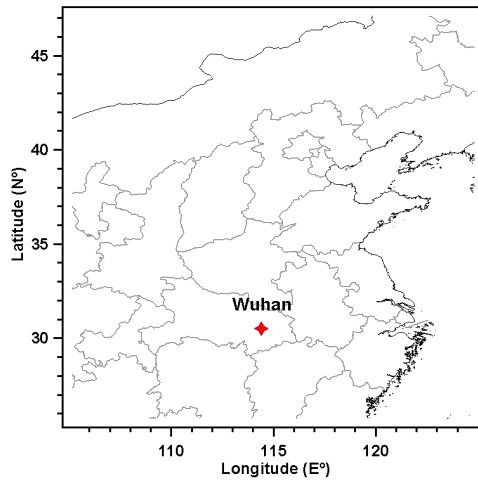
58 The method detection limit (MDL) and measurement uncertainties (MU%) are employed to calculate the uncertainty of each
59 sample based on the following equations:

$$60 \quad U_{ij} = \sqrt{(MU \times concentration)^2 + (1/2MDL)^2} \quad (3)$$

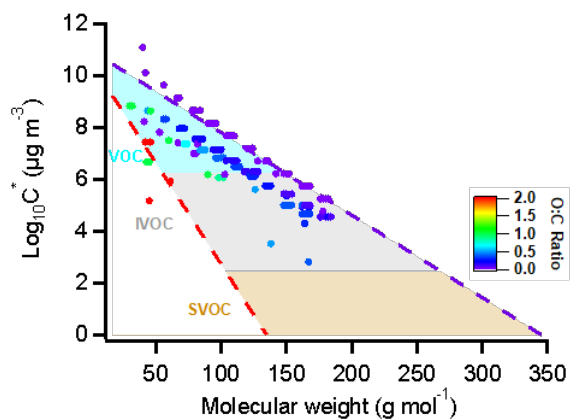
$$61 \quad U_{ij} = \frac{5}{6} \times MDL \quad (4)$$

62 When the species concentration is higher than its MDL, Eq. (3) is used to calculate the uncertainty. Otherwise, Eq. (4) is used.

63



64
65 **Figure S1: Location of the observation region and sampling site. (The right figure is from © Google Maps.)**
66



67
 68 **Figure S2: Molecular corridors (vapor saturation pressure at 25°C, C^* , as a function of molecular weight) for the**
 69 **compounds measured by the PTR-ToF-MS in this work, colored by the O:C ratio. Below and above $\text{log}C^*=6.5$ and 2.5**
 70 **(in $\mu\text{g m}^{-3}$) is defined as intermediate-volatile and volatile organic compounds, respectively.**
 71

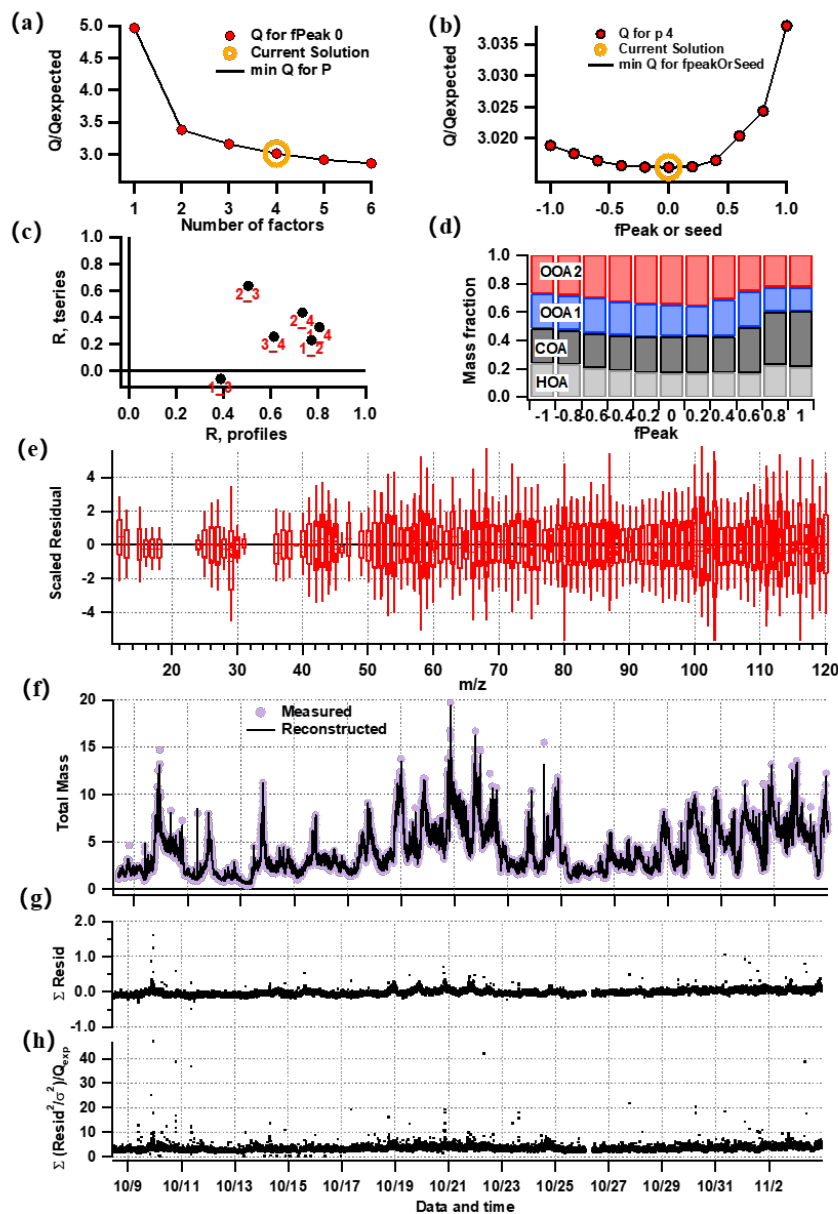
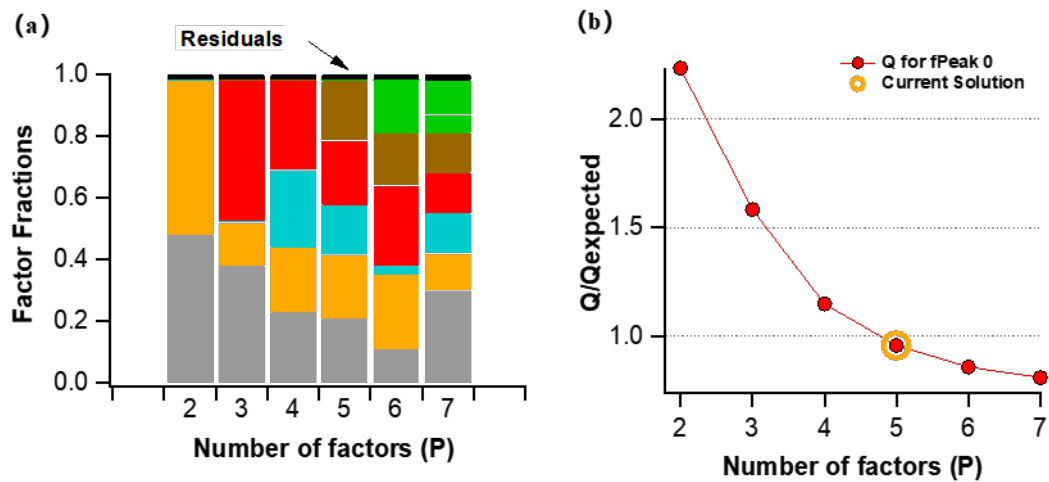


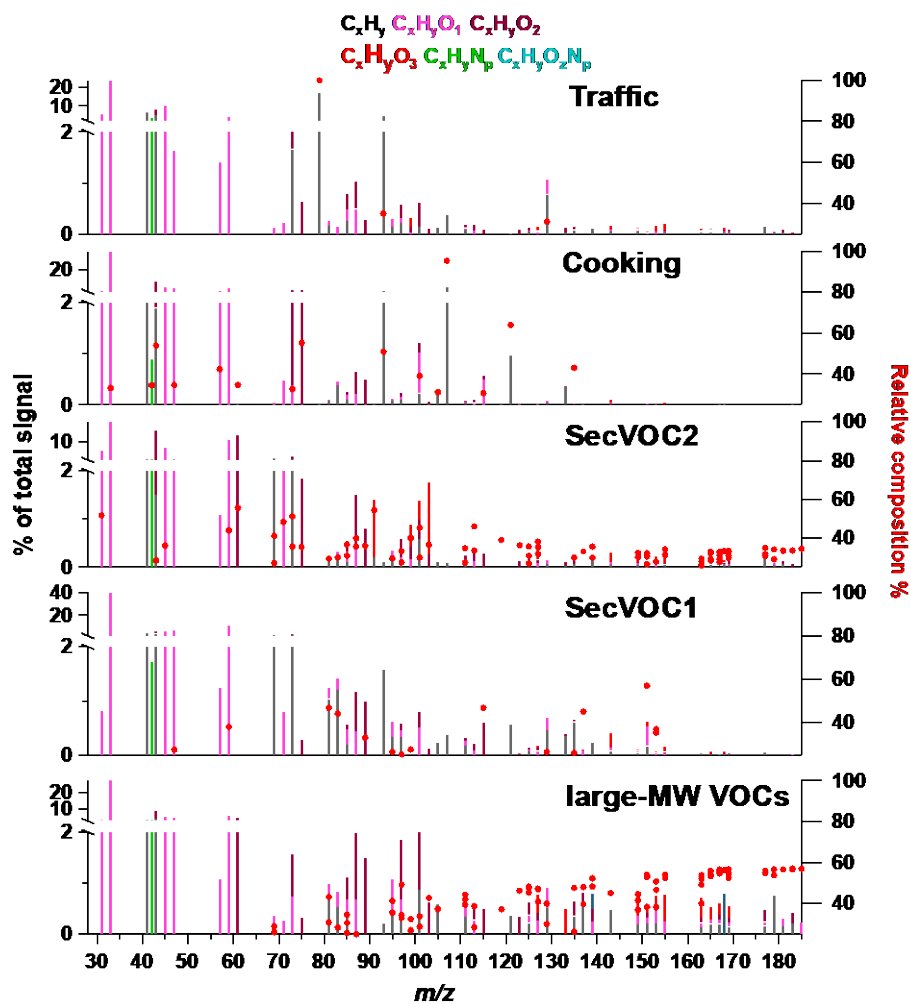
Figure S3: A summary of PMF diagnostic plot: (a) Q/Q_{exp} as a function of number of factors; (b) Q/Q_{exp} as a function of f_{Peak} value; (c) correlations of the time series and spectral profiles among the PMF factors; (d) mass fraction of OA factors as a function of f_{peak} ; (e) scaled residual for each fragment ion; (f) comparison of measured and PMF reconstructed mass; (g) time series of residual, and (h) time series of Q/Q_{exp} values.

72
73
74
75
76
77
78



79
80
81
82
83

Figure S4: Q/Q_{exp} values as a function of factor number in PMF (a); factor fractions from various factors in different PMF solutions (b).



84
85
86
87
88
89

Figure S5: Source attributed VOCs measured by the PTR-TOF-MS (a-e). Mass profiles of the five factors resolved of PMF (traffic VOCs, cooking VOCs, secondary VOCs (SecVOC2, SecVOC1) and large molecular weight (MW) VOCs (large-MW VOCs), with major relative composition contribution labeled in the mass spectra.

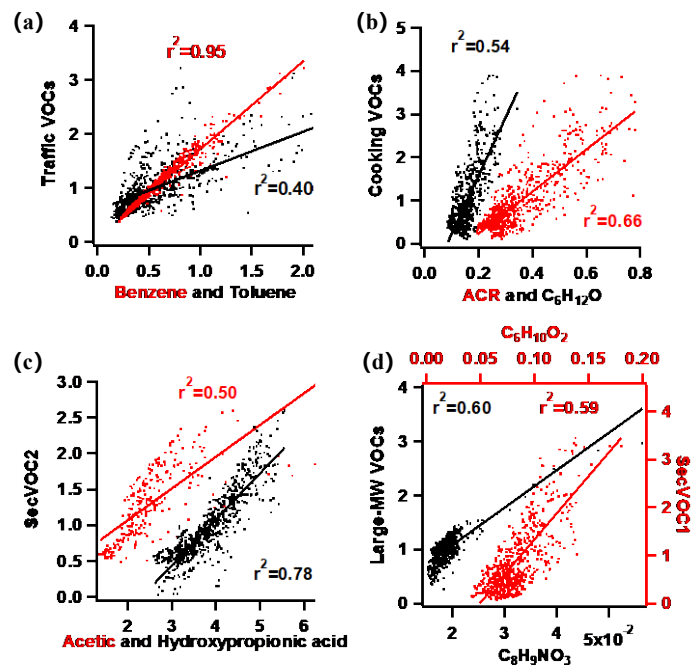
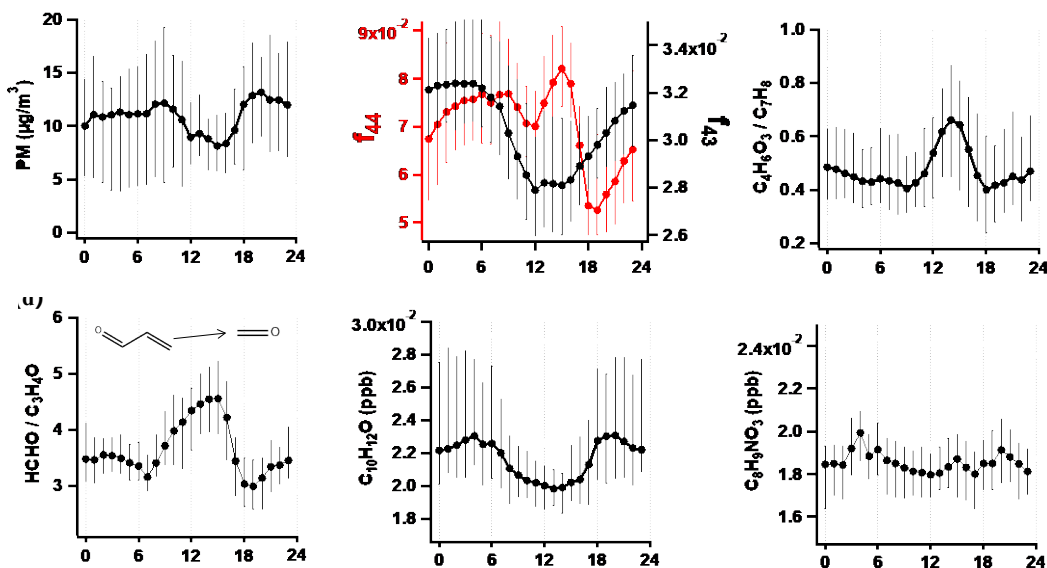


Figure S6: The scatter plots between VOCs factors and tracer species (ppb).



94
 95 **Figure S7: Diurnal variations of: (a) total PM concentration measured by SMPS; (b) f_{44} (left) and f_{43} (right); (c-f)**
 96 **involved species both during photo- and dark oxidation.**
 97

98 **References**

99 Cappellin, L., Karl, T., Probst, M., Ismailova, O., Winkler, P., Soukoulis, C., Aprea, E., Märk, T., Gasperi, F., and Biasioli, F.: On Quantitative
 100 Determination of Volatile Organic Compound Concentrations Using Proton Transfer Reaction Time-of-Flight Mass Spectrometry, *Environ.*
 101 *Sci. Technol.*, 46, 2283-2290, <https://doi.org/10.1021/es203985t>, 2012.
 102 Hartikainen, A., Yli-Pirilä, P., Tiitta, P., Leskinen, A., Kortelainen, M., Orasche, J., Schnelle-Kreis, J., Lehtinen, K., Zimmermann, R.,
 103 Jokiniemi, J., and Sippula, O.: Volatile Organic Compounds from Logwood Combustion: Emissions and Transformation under Dark and
 104 Photochemical Aging Conditions in a Smog Chamber, *Environ. Sci. Technol.*, 52, 4979–4988, <https://doi.org/10.1021/acs.est.7b06269>,
 105 2018.
 106 Zhang, Q., Jimenez, J., Canagaratna, M., Ulbrich, I., Ng, N., Worsnop, D., and Sun, Y.: Understanding atmospheric organic aerosols via
 107 factor analysis of aerosol mass spectrometry: a review, *Anal. Bioanal. Chem.*, 401, 3045-3067, <https://doi.org/10.1007/s00216-011-5355-y>,
 108 2011.
 109